Cover Sheet

Authors: Tongfei Li, Sulin Li, Qianyu Liu, Yechao Tian, Yiwei Zhang, Gengtao Fu, Yawen Tang

Title: Hollow Co_3O_4/CeO_2 Heterostructure *In-situ* Embedded in N-doped Carbon Nanofibers Enable Outstanding Oxygen Evolution

Number of pages and figures in the manuscript was 28 and 6, respectively.

Number of pages, figures, and tables in the supporting information was 16, 9, and 1, respectively.

Supporting Information

Hollow Co_3O_4/CeO_2 Heterostructure In-situ Embedded in N-doped Carbon Nanofibers Enable Outstanding Oxygen Evolution

Tongfei Li,[†,‡] Sulin Li,[‡] Qianyu Liu,[‡] Yechao Tian, [‡] Yiwei Zhang,[†,*] Gengtao Fu,[§,*] Yawen Tang[‡,*]

[†] School of Chemistry and Chemical Engineering, Southeast University, Jiangsu Optoelectronic Functional Materials and Engineering Laboratory, No. 2, Southeast University Road, Nanjing 211189, China

[‡] Jiangsu Key Laboratory of New Power Batteries, Jiangsu Collaborative Innovation Centre of Biomedical Functional Materials, School of Chemistry and Materials Science, Nanjing Normal University, No. 1, Wenyuan Road, Nanjing 210023, China

[§] School of Chemical and Biomedical Engineering, Nanyang Technological University, 62 Nanyang Dr, Singapore 637459, Singapore

*E-mail: zhangchem@seu.edu.cn (Y.Z); gengtaofu@gmail.com (G. F.); tangyawen@njnu.edu.cn (Y. T.)

Experimental section

Materials: Cobalt (II) nitrate hexahydrate ($Co(NO_3)_2 \cdot 6H_2O$), Cerium (III) nitrate hexahydrate ($Ce(NO_3)_3 \cdot 6H_2O$) and Polyvinyl pyrrolidone (PVP, *M*w ≈ 1 300 000) were obtained from Alfa Aesar. N, N-dimethylformamide (DMF), ethanol (C_2H_5OH) were purchased from Sinopharm Chemical Reagent Co., Ltd. All chemical reagents were used as received without further purification.

Synthesis of h-Co_3O_4/CeO_2@N-CNFs: For a typical procedure, 1.0 g PVP, 1.0 mmol $Co(NO_3)_2 \cdot 6H_2O$ and 0.5 mmol $Ce(NO_3)_3 \cdot 6H_2O$ is added with 12 mL DMF and stirred at ambient condition for the overnight. Afterward, the homogeneous solution filled into 10 mL plastic syringe equipped with a 22-gauge needle tip, the distance between the anode (needle tip) and the cathode (aluminum foil as the collector) is 18 cm and a DC voltage of 20 KV was applied in the electrospinning set up. The as-obtained nanofiber membrane was initially stabilized at 250 ºC for 3 h in open air, subsequently by the annealing at 600 ºC for carbonization for 3 h in N_2 atmosphere at a rate of 5 ºC/min to synthesize the final h-Co_3O_4/CeO_2@N-CNFs. Similarly, the Co_3O_4@N-CNFs and CeO_2@N-CNFs were prepared without involvement of cerium and cobalt precursors, respectively. In addition, the N-CNFs is prepared from PVP without introducing any metal sources.

Structure and Morphology Characterizations: X-ray diffraction (XRD) patterns were obtained on a Model D/max-rC X-ray diffractometer with Cu Kα radiation (λ = 1.5406 Å). Transmission electron microscopy (TEM), High-resolution TEM (HRTEM) and Field-emission scanning electron microscopy (FESEM) were performed on a JEOL

JEM-2100F with an accelerating voltage of 200 kV and JEOL JSM7500F, respectively. High-angle annular dark-field scanning TEM (HAADF-STEM) images, Elemental mapping images and electron energy dispersive spectroscopy (EDS) were conducted on FEI Tecnai G2 F20 microscope, with an accessory built on the JEOL JEM-2100F. Thermogravimetric analysis (TGA) was measured on a NetzschSTA449C thermal analyzer with a ramp rate of 10 °C min^{-1} under air atmosphere. The X-ray photoelectron spectroscopy (XPS) was recorded on a Thermo VG Scientific ESCALAB 250 spectrometer with an Al Kα radiator. The Raman spectra were received on a Raman spectrometer (Lab RAM HR800, λ = 514 nm). N_2 adsorption and desorption test, and the corresponding Brunauer-Emmett-Teller (BET) surface area, pore diameter were displayed on Micromeritics ASAP 2050 instrument.

Electrochemical measurements: The OER measurements were performed on a CHI 760E workstation taking a conventional three-electrode system. A graphite rod was served as the counter electrode, while a glassy carbon electrode (d = 5 mm) and saturated calomel electrode (SCE) worked as the working and reference electrode, respectively. To prepared the working electrode, 4.0 mg catalyst were ultrasonically dispersed for 30 min in a mixture solvent containing 1.2 mL H_2O, 0.6 mL C_2H_5OH and 0.2 mL Nafion (5 wt%) solution. Afterward, 20 μL of the sample suspension was dropped onto the polished glassy carbon electrode surface gradually and then dried at room temperature. Hereafter, the working electrode with catalyst-loaded was obtained. All the electrochemical measurements were performed in 0.1 M KOH media. Specifically, the Linear Scanning Voltammogram (LSV) plots were performed in O_2-

saturated 0.1 M KOH electrolyte with a rotation speed of 1600 rpm at a scan rate of 5 mV s^{-1}, after the O_2 was purged into the electrolyte for 30 min to make the solution full of O_2 gas. The Cyclic Voltammetry (CV) was conducted in O_2-saturated electrolyte with a scan rate of 5 mV s^{-1}. All potentials in this work were transformed into potentials versus reversible hydrogen electrode (RHE), and follow the equation as following: $E_{RHE} = E_{SCE} + 0.0592\ pH + 0.242$. The C_{dl} calculation according to the following expression: $C_{dl} = (ja - jc)/(2*v) = (ja + |jc|)/(2*v) = \Delta j/(2*v)$, where ja and jc are the anodic and cathodic voltammetric current density, respectively, and v is the scan rate.

Figures and Table

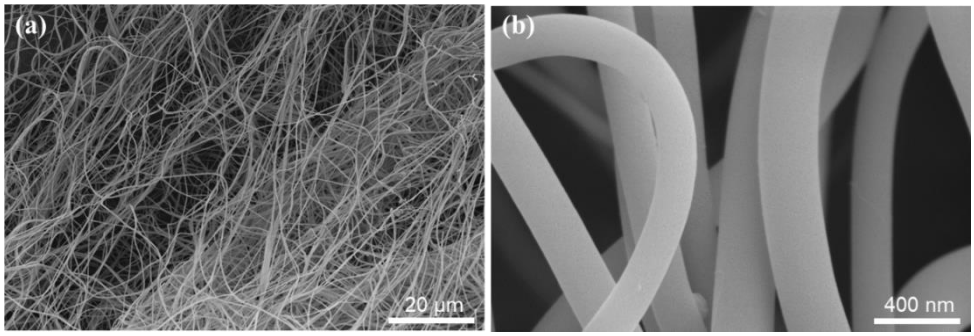

Figure S1. (a and b) SEM images of the as-spun precursor nanofibers with different magnifications.

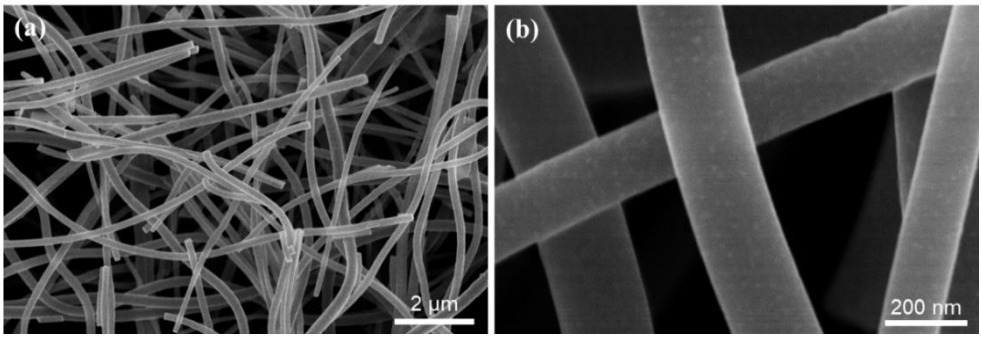

Figure S2. (a and b) SEM images of h-Co_3O_4/CeO_2@N-CNFs with different magnifications.

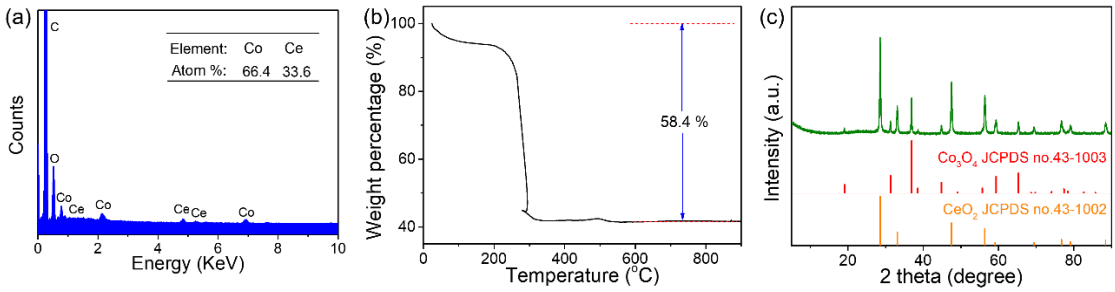

Figure S3. Compositional examinations of h-Co_3O_4/CeO_2@N-CNFs: (a) EDS spectrum, (b) TGA curve and (c) XRD pattern after TGA measurement.

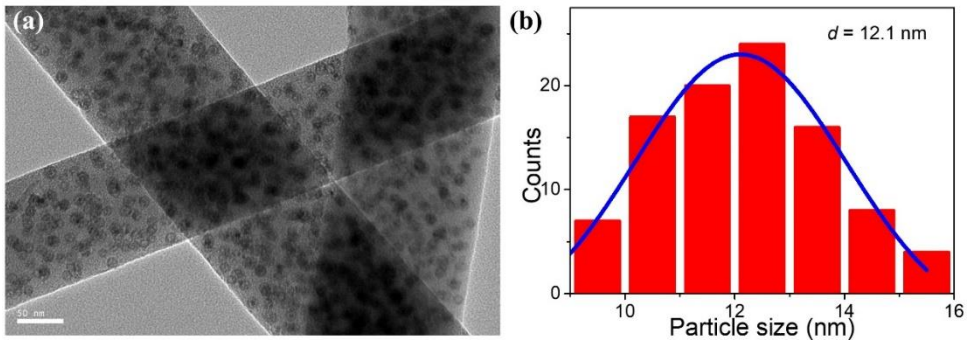

Figure S4. (a) Typical TEM image of the fabricated h-Co_3O_4/CeO_2@N-CNFs; (b) particle size distribution of the embedded Co_3O_4/CeO_2 nanoparticles.

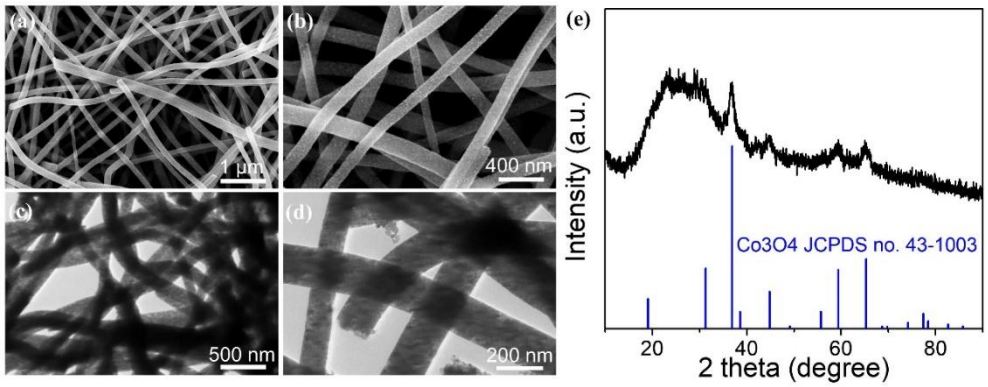

Figure S5. (a and b) SEM images, (c and d) TEM images and (e) XRD pattern of the synthesized Co_3O_4@N-CNFs.

For the synthesized Co_3O_4@N-CNFs, SEM images (Figure S5a, b) and TEM images (Figure S5c, d) suggest that the resultant Co_3O_4@N-CNFs exhibited similar structural features with the standard h-Co_3O_4/CeO_2@N-CNFs, *i. e.* fiber-like nanostructure, randomly oriented and highly interconnected. Meantime, the Co_3O_4 nanoparticles are uniform distributed on the surface of N-doped carbon nanofibers. The XRD pattern (Figure S5e) indicates its composition of spinel-phased Co_3O_4.

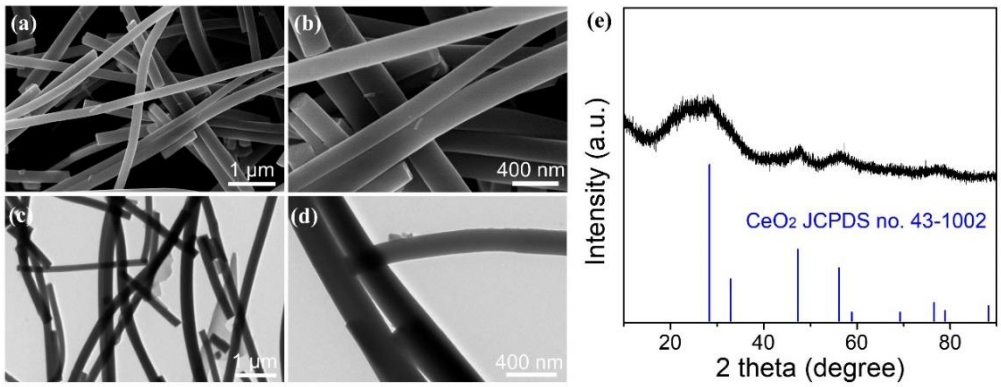

Figure S6. (a and b) SEM images, (c and d) TEM images and (e) XRD pattern of the synthesized CeO_2@N-CNFs.

For the as-prepared CeO_2@N-CNFs, SEM images (Figure S6a, b) and TEM images (Figure S6c, d) with different magnifications demonstrate that the as-spun product is made of 1D nanofibers with smooth surface and uniform diameter of ~ 200 nm, the CeO_2 nanoparticles are close encased within the N-doped carbon nanofibers. XRD pattern (Figure S6e) shows the typical diffraction peak at around 25°, which can be indexed to (002) plane of the graphitic carbon. While the other peaks perfectly related to cubic CeO_2 (JCPDS no.43-1002).

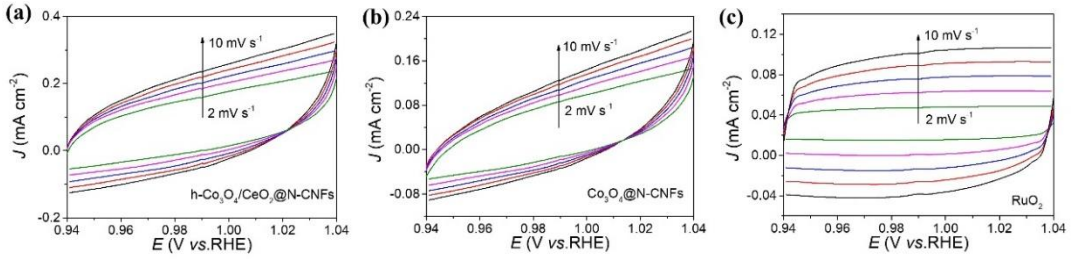

Figure S7. CV curves of the synthesized catalysts in the non-Faradaic region (0.94 – 1.04 V *vs* RHE) obtained at different scanning rates. (a) standard h-Co_3O_4/CeO_2@N-CNFs, (b) Co_3O_4@N-CNFs, and (c) commercial RuO_2 catalyst.

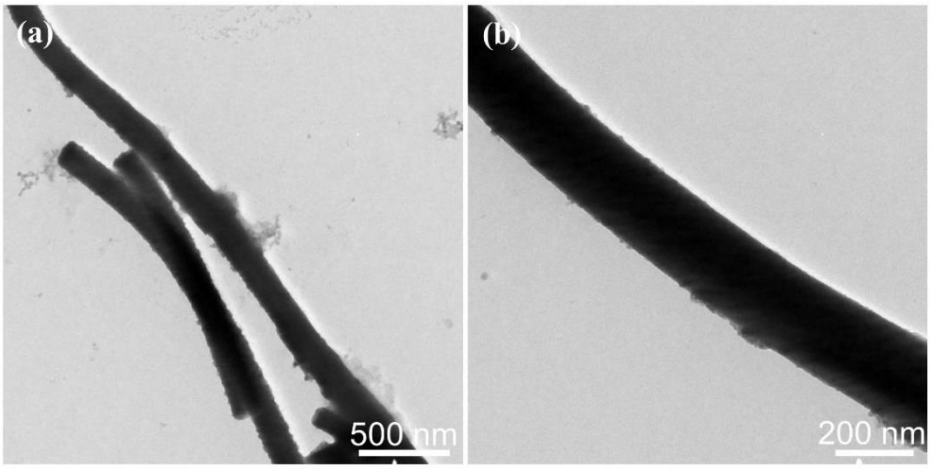

Figure S8. TEM images of the h-Co_3O_4/CeO_2@N-CNFs after the durability test.

Table S1. Comparison of the OER activities of the as-synthesized h-Co_3O_4/CeO_2@N-CNFs with recently reported noble-metal-free electrocatalysts in alkaline solution.

Catalyst	Overpotential / mV ($10\ mA\ cm^{-2}$)	Tafel slop ($mV\ dec^{-1}$)	Electrolyte	Ref
Ce-NiO	382	118.7	1.0 M KOH	S1
CeO_x/CoO_x	331	66	1 M NaOH	S2
Co_3O_4/$NiCo_2O_4$ DSNCs	~400	110	1.0 M KOH	S3
$CoFe_2O_4$/G	460	N/A	0.1 M KOH	S4
$CoFe_2O_4$@N-CNFs	349	80	0.1 M KOH	S5
Co_3O_4 nanotubes	390	76	0.1 M KOH	S6
$Co_{0.5}Fe_{0.5}S$@N-MC	410	159	1.0 M KOH	S7
CoCH/NF	332	126	1.0 M KOH	S8
NiCoP/C nanoboxes	330	96	1.0 M KOH	S9
Co_3ZnC/Co@CN	366	81	1.0 M KOH	S10
Co@NCNT	429	116	1.0 M KOH	S11
Co/CoP-5	340	79.5	1.0 M KOH	S12
SSUCo-900	337	N/A	1.0 M KOH	S13
Cl-doped $Co(OH)_2$	330	98	1.0 M KOH	S14
Co-N/GFs-700	313	N/A	1.0 M KOH	S15
Ce-$MnCo_2O_4$-3%	390	125	1.0 M KOH	S16
Co-CeO_2/N-CNR	410	90	0.1 M KOH	S17
$NiPS_3$@NiOOH	350	80	0.1 M KOH	S18
Co_3O_4/N-CNTA	432	79.65	0.1 M KOH	S19
$NiCo_2O_4$@Ni-Co-Ci	309	91	1.0 M KOH	S20
h-Co_3O_4/CeO_2@N-CNFs	**310**	**85**	**0.1 M KOH**	**This work**

References

[S1] Gao, W.; Xia, Z.; Cao, F.; Ho, J. C.; Jiang, Z.; Qu, Y. Comprehensive Understanding of the Spatial Configurations of CeO_2 in NiO for the Electrocatalytic Oxygen Evolution Reaction: Embedded or Surface-Loaded. *Adv. Funct. Mater.* **2018,** *28*, 1706056.

[S2] Kim, J.-H.; Shin, K.; Kawashima, K.; Youn, D. H.; Lin, J.; Hong, T. E.; Liu, Y.; Wygant, B. R.; Wang, J.; Henkelman, G.; Mullins, C. B. Enhanced Activity Promoted by CeO_x on a CoO_x Electrocatalyst for the Oxygen Evolution Reaction. *ACS Catal.* **2018,** *8*, 4257-4265.

[S3] Hu H.; Guan B.; Xia B.; Lou X. Designed Formation of Co_3O_4/$NiCo_2O_4$ Double-Shelled Nanocages with Enhanced Pseudocapacitive and Electrocatalytic Properties. *J. Am. Chem. Soc.*, **2015,** *137*, 5590-5595.

[S4] Bian W.; Yang Z.; Strasser P.; Yang R. A $CoFe_2O_4$/graphene nanohybrid as an efficient bi-functional electrocatalyst for oxygen reduction and oxygen evolution. *J. Power Sources*, **2014,** *250*, 196-203.

[S5] Li, T.; Lv, Y.; Su, J.; Wang, Y.; Yang, Q.; Zhang, Y.; Zhou, J.; Xu, L.; Sun, D.; Tang, Y. Anchoring $CoFe_2O_4$ Nanoparticles on N-Doped Carbon Nanofibers for High-Performance Oxygen Evolution Reaction. *Adv. Sci.* **2017,** *4*, 1700226.

[S6] Wang H.; Zhuo S.; Liang Y.; Han X.; Zhang B. General Self-template Synthesis of Transition Metal Oxide and Chalcogenide Mesoporous Nanotubes with Enhanced Electrochemical Performances. *Angew. Chem. Int. Ed.* **2016,** *55*, 9055-9059.

[S7] Shen M.; Ruan C.; Chen Y.; Jiang C.; Ai K.; Lu L. Covalent entrapment of cobalt-iron sulfides in N-doped mesoporous carbon: extraoridinary bifunctional electrocatalysts for oxygen reduction and evolution reactions. *ACS Appl. Mater. Interfaces* **2015,** *7*, 1207-1218.

[S8] Xie M.; Yang L.; Ji Y.; Wang Z.; Ren X.; Liu Z.; Asiri A. M.; Xiong X.; Sun X. An amorphous Co-carbonate-hydroxide nanowire array for efficient and durable oxygen evolution reaction in carbonate electrolytes. *Nanoscale*, **2017,** *9*, 16612-16615.

[S9] He P.; Yu X. Y.; Lou X. W. Carbon-Incorporated Nickel–Cobalt Mixed Metal

Phosphide Nanoboxes with Enhanced Electrocatalytic Activity for Oxygen Evolution. *Angew. Chem., Int. Ed.*, **2017,** *56*, 3897-3911.

[S10] Su J.; Xia G.; Li R.; Yang Y.; Chen J.; Shi R.; Jiang P.; Chen Q. Co_3ZnC/Co nano heterojunctions encapsulated in N-doped graphene layers derived from PBAs as highly efficient bi-functional OER and ORR electrocatalysts. *J. Mater. Chem. A*, **2016,** *4*, 9204-9212.

[S11] Zhang E.; Xie Y.; Ci S.; Jia J.; Cai P.; Yi L.; Wen Z. Multifunctional high-activity and robust electrocatalyst derived from metal-organic frameworks. *J. Mater. Chem. A*, **2016**, *4*, 17288-17298.

[S12] Xue Z.-H.; Su H.; Yu Q.-Y.; Zhang B.; Wang H.-H.; Li X.-H.; Chen J.-S. Janus Co/CoP Nanoparticles as Efficient Mott–Schottky Electrocatalysts for Overall Water Splitting in Wide pH Range. *Adv. Energy Mater*., **2017**, *7*, 1602355.

[S13] Zhang G.; Wang P.; Lu W.T.; Wang C.Y.; Li Y.K.; Ding C.; Gu J.; Zheng X.S.; Cao F.F. Co Nanoparticles/Co, N, S Tri-doped Graphene Templated from In-Situ-Formed Co, S Co-doped g-C_3N_4 as an Active Bifunctional Electrocatalyst for Overall Water Splitting. *ACS Appl. Mater. Interfaces*, **2017**, *9*, 28566-28576.

[S14] Kou Y.; Liu J.; Li Y.; Qu S.; Ma C.; Song Z.; Han X.; Deng Y.; Hu W.; Zhong C. Electrochemical Oxidation of Chlorine-Doped $Co(OH)_2$ Nanosheet Arrays on Carbon Cloth as a Bifunctional Oxygen Electrode. *ACS Appl. Mater. Interfaces*. **2018**, *10*, 796-805.

[S15] Tong Y.; Yu X.; Wang H.; Yao B.; Li C.; Shi G. Trace Level Co−N Doped Graphite Foams as High-Performance Self-Standing Electrocatalytic Electrodes for Hydrogen and Oxygen Evolution. *ACS Catal.*, **2018**, *8*, 4637-4644.

[S16] Huang, X.; Zheng, H.; Lu, G.; Wang, P.; Xing, L.; Wang, J.; Wang, G. Enhanced Water Splitting Electrocatalysis over $MnCo_2O_4$ via Introduction of Suitable Ce Content. *ACS Sustain. Chem. Eng.* **2018,** *7*, 1169-1177.

[S17] Sivanantham, A.; Ganesan, P.; Shanmugam, S. A synergistic effect of Co and CeO_2 in nitrogen-doped carbon nanostructure for the enhanced oxygen electrode activity and stability. *Appl. Catal. B-Environ.* **2018,** *237*, 1148-1159.

[S18] Konkena B.; Masa J.; Botz A. J. R.; Sinev I.; Xia W.; Koßmann J.; Drautz R.; Muhler M.; Schuhmann W. Metallic $NiPS_3$@NiOOH Core−Shell Heterostructures as Highly Efficient and Stable Electrocatalyst for the Oxygen Evolution Reaction. *ACS Catal.*, **2017,** *7*, 229-237.

[S19] Tian W.; Li H.; Qin B.; Xu Y.; Hao Y.; Li Y.; Zhang G.; Liu J.; Sun X.; Duan X. Tuning the wettability of carbon nanotube arrays for efficient bifunctional catalysts and Zn–air batteries. *J. Mater. Chem. A* **2017,** *5*, 7103-7110.

[S20] Ge R.; Ma M.; Ren X.; Qu F.; Liu Z.; Du G.; Asiri A. M.; Chen L.; Zheng B.; Sun X. A $NiCo_2O_4$@Ni–Co–Ci core–shell nanowire array as an efficient electrocatalyst for water oxidation at near-neutral pH. *Chem. Commun.* **2017**, *53*, 7812-7815.